

A nonlinear wave coupling algorithm and its programing and application in plasma turbulences

Yong Shen(沈勇), Yu-Hang Shen(沈煜航), Jia-Qi Dong(董家齐), Kai-Jun Zhao(赵开君), Zhong-Bing Shi(石中兵), and Ji-Quan Li(李继全)

Citation: Chin. Phys. B, 2022, 31 (**6**): 065206. DOI: 10.1088/1674-1056/ac4233
Journal homepage: http://cpb.iphy.ac.cn; http://iopscience.iop.org/cpb

What follows is a list of articles you may be interested in

ISSDE: A Monte Carlo implicit simulation code based on Stratonovich SDE approach of Coulomb collision

Yifeng Zheng(郑艺峰), Jianyuan Xiao(肖建元), Yanpeng Wang(王彦鹏), Jiangshan Zheng(郑江山), and Ge Zhuang(庄革)
Chin. Phys. B, 2021, 30 (**9**): 095201. DOI: 10.1088/1674-1056/abefc7

Energy behavior of Boris algorithm

Abdullah Zafar and Majid Khan
Chin. Phys. B, 2021, 30 (**5**): 055203. DOI: 10.1088/1674-1056/abd161

Analysis of asymmetry of the D_α emission spectra under the Zeeman effect in boundary region for D-D experiment on EAST tokamak

Wei Gao(高伟), Juan Huang(黄娟), Jianxun Su(宿建勋), Jing Fu(付静), Yingjie Chen(陈颖杰), Wei Gao(高伟), Zhenwei Wu(吴振伟), and EAST Team
Chin. Phys. B, 2021, 30 (**2**): 025201. DOI: 10.1088/1674-1056/abc162

Reversed rotation of limit cycle oscillation and dynamics of low-intermediate-high confinement transition

Dan-Dan Cao(曹丹丹), Feng Wan(弯峰), Ya-Juan Hou(侯雅娟), Hai-Bo Sang(桑海波), Bai-Song Xie(谢柏松)
Chin. Phys. B, 2018, 27 (**6**): 065201. DOI: 10.1088/1674-1056/27/6/065201

A radial non-uniform helicon equilibrium discharge model

Cheng Yu-Guo, Cheng Mou-Sen, Wang Mo-Ge, Li Xiao-Kang
Chin. Phys. B, 2014, 23 (**10**): 105202. DOI: 10.1088/1674-1056/23/10/105202

A nonlinear wave coupling algorithm and its programing and application in plasma turbulences

Yong Shen(沈勇)[1,†], Yu-Hang Shen(沈煜航)[2], Jia-Qi Dong(董家齐)[3,1], Kai-Jun Zhao(赵开君)[4], Zhong-Bing Shi(石中兵)[1], and Ji-Quan Li(李继全)[1]

[1] *Southwestern Institute of Physics, Chengdu* 610041, *China*
[2] *School of Information and Communication Engineering, University of Electronic Science and Technology of China, Chengdu* 611731, *China*
[3] *Institute for Fusion Theory and Simulation, Zhejiang University, Hangzhou* 310013, *China*
[4] *College of Nuclear Science and Engineer, East China University of Technology, Nanchang* 330013, *China*

(Received 8 September 2021; revised manuscript received 1 December 2021; accepted manuscript online 11 December 2021)

The fully developed turbulence can be regarded as a nonlinear system, with wave coupling inside, which causes the nonlinear energy to transfer, and drives the turbulence to develop further or be suppressed. Spectral analysis is one of the most effective methods to study turbulence system. In order to apply it to the study of the nonlinear wave coupling process of edge plasma turbulence, an efficient algorithm based on spectral analysis technology is proposed to solve the nonlinear wave coupling equation. The algorithm is based on a mandatory temporal static condition with the nonideal spectra separated from the ideal spectra. The realization idea and programing flow are given. According to the characteristics of plasma turbulence, the simulation data are constructed and used to verify the algorithm and its implementation program. The simulation results and experimental results show the accuracy of the algorithm and the corresponding program, which can play a great role in the studying the energy transfer in edge plasma turbulences. As an application, the energy cascade analysis of typical edge plasma turbulence is carried out by using the results of a case calculation. Consequently, a physical picture of the energy transfer in a kind of fully developed turbulence is constructed, which confirms that the energy transfer in this turbulent system develops from lower-frequency region to higher-frequency region and from linear growing wave to damping wave.

Keywords: bispectral analysis, wave coupling, algorithm, plasma turbulence, energy cascade

PACS: 52.65.–y, 52.35.Ra, 52.35.–g **DOI:** 10.1088/1674-1056/ac4233

1. Introduction

Digital bispectral analysis method can be applied to the studying of fluid turbulence,[1] plasma saturated turbulence,[2–5] and other nonlinear systems, which has proved to be a very important data analysis technology in practice. In the late 1980s, Ritz *et al*. studied this problem and presented an algorithm using bispectral analysis technique.[6–8] In the Ritz *et al*.'s method the iterative technique is used to solve the wave coupling equation, but the fourth-order moment in the equation is approximated by a second-order moment. The input signals can be non-Gaussian signals or Gaussian signals. The typical application of this method is to deal with the transiting flow.[7] Using the Ritz *et al*.'s algorithm, one can use experimental turbulence data to quantitatively estimate nonlinear coupling coefficients or estimate the magnitude of energy cascades between waves in a fully developed turbulence system. However, because in the Ritz *et al*.'s method, the authors did not take into consideration the non-ideal fluctuations, the calculation results tend to have large systematic errors and often produce large non-physical damping coefficients.

In order to make up for the defects of Ritz *et al*'s method, Kim *et al*. reconstructed the power spectrum by retaining the role of the fourth moment and proposed Kim *et al*.'s algorithm in 1996,[9] where the spectrum is divided into ideal spectrum component and non-ideal spectrum component, and the spectrum components directly related to the quadratic nonlinear interaction are called ideal spectrum, while the non-ideal spectrum does not participate in the linear coupling process nor the tree-wave coupling process. Kim *et al*.'s method imposes a time-static condition of "input ideal spectral power equals output ideal spectral power" to include an assumption of local homogeneity.

Nevertheless, in some nonlinear systems such as developing turbulent systems such as shallow ocean waves, the assumption of Kim *et al*.'s algorithm may not hold. In such systems, forcing the power of the input spectrum to equal that of the output spectrum would lose a lot of valid information. In this respect, Kim proposed the linear regression method and successfully solved such problems.[10] In the process of studying such systems, in Ref. [11] the authors proposed another new digital bispectral analysis algorithm — complete iterative method — to calculate and analyze the three-wave interaction inside the developing turbulence. The complete iteration method is an extension of Ritz method, while it contains the effect of the fourth moment in the wave coupling equation, so that all the wave information has been considered. In Ref. [11], the applicability of complete iterative method in fluid turbulence was discussed in detail, however, the application prospect of this method in plasma has not been analyzed

[†]Corresponding author. E-mail: sheny@swip.ac.cn

© 2022 Chinese Physical Society and IOP Publishing Ltd

yet. Subsequently, the study of Ref. [12] focused on this issue and made the comparative analysis of the performance of the complete iteration method and Kim method, and studied the applicability of these two mainstream algorithms in edge plasma turbulence spectrum analysis. The results show that the spectral characteristics of edge plasma turbulence are different from those of fluid turbulence. That is, in the edge plasmas, the energy mainly concentrates in the low-frequency region, and the high-order coupling may occupy a certain proportion, which needs to be eliminated from the three-wave coupling effect, which can be done by employing the Kim hypothesis.

According to the above results, Kim's algorithm is shown suitable to be used in the study of edge plasma turbulence. It is of significant importance for the study of the energy transfers occurring in fully developed turbulent system due to nonlinear properties of the flows, and the wave coupling equation describing the changes of spectral components has representative significance in such nonlinear systems. However, none of the previous studies has involved the specific program implementation with respect to this algorithm, although it is indeed an important topic. Shen *et al*. carried out this kind of work in advance.[13,14] In Ref. [14], an algorithm and its programming for solving the wave coupling equation were presented, while the algorithm still belongs to a kind of linear regression analysis methods, therefore, its structure turns relatively complex. In this work, an algorithm and program based on Kim *et al*.'s method are developed to solve the nonlinear wave coupling equations, in which the Kim's hypothesis is completely adopted. The algorithm has simpler structure and higher precision. This work focuses on realizing the idea, the programming and simulation-verifying the algorithm, thereby improving the work of Ref. [11] and providing a feasible software tool for studying the plasma turbulence.

2. Modeling and algorithm implementation

2.1. Physical and mathematical model

In sea waves and some other wave systems, the input and output signals are given, and the output signals can be generated through linear transformation process and nonlinear transformation process.[15,16] Such a system can be seen as a "black box". If only linear transformation process and quadratic nonlinear transformation process are considered, and the cubic and higher order nonlinear processes are weak, the nonlinear system can be expressed by the following nonlinear transfer equation:

$$Y_f = L_f X_f + \frac{1}{2} \sum_{\substack{f_1,f_2 \\ f=f_1+f_2}} Q_f^{f_1,f_2} X_{f_1} X_{f_2} + \varepsilon_f. \tag{1}$$

Here, X_f and Y_f represent input and output signal spectra, respectively. And L_f and $Q_f^{f_1,f_2}$ are named linear transfer function and nonlinear transfer function, respectively, and ε_f is the error item. It is worthy to note that for quadratic nonlinearity, the process is three-wave coupling. In the process of Fourier decomposition with wave vector k and frequency f, waves (or modes) can interact with each other, satisfying the constraint condition that $k = k_1 + k_2$ and $f = f_1 + f_2$, *i.e.*, two waves of wave number k_1 (frequency f_1) and k_2 (frequency f_2) are coupled to generate a wave of wave number k (frequency f), or *vice versa*. If L_f and $Q_f^{f_1,f_2}$ are obtained by solving Eq. (1), the black box can thus be described precisely. The schematic of the nonlinear system is shown in Fig. 1.

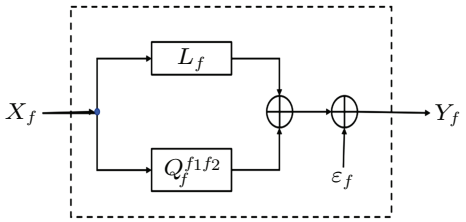


Fig. 1. Schematic model of nonlinear system.

On the other hand, in order to quantitatively estimate the linear growth rate of fully developed turbulence and the energy cascade between waves, we consider the nonlinear drift wave coupling equation in the following form:

$$\begin{aligned} \frac{\partial \phi(f,x)}{\partial x} &= \Lambda_f^L \phi(f,x) + \frac{1}{2} \sum_{\substack{f_1,f_2 \\ f=f_1+f_2}} \Lambda_f^Q(f_1,f_2)\,\phi(f_1,x)\,\phi(f_2,x) \\ &= \Lambda_f^L \phi(f,x) + \sum_{\substack{f_1 \geq f_2 \\ f=f_1+f_2}} \Lambda_f^Q(f_1,f_2)\,\phi(f_1,x)\,\phi(f_2,x), \end{aligned} \tag{2}$$

where $\phi(f,x)$ is the signal spectrum at frequency f, with x being the distance between the spatial locations where the input and output signals are measured, Λ_f^L is linear coupling coefficient, and Λ_f^Q is quadratic nonlinear coupling coefficient. The governing equation (2) describes turbulence determined by three-wave coupling, indicating that the change of spatial Fourier spectrum in wave field is determined only by linear interaction and quadratic nonlinear interaction.[17–23] Noting that here the wave-number space has been transformed into the frequency space.[24] The coefficient Λ_f^L includes linear damping and growth, spectral broadening (linear dispersion), and diamagnetic drift term. The quadratic nonlinear coupling coefficient Λ_f^Q gives the strength of the mode coupling due to the convective derivative terms such as the nonlinear polarization drift and the $\boldsymbol{E} \times \boldsymbol{B}$ convection of density in the drift wave model.[4]

Spectrum $\phi(f,x)$ is a complex number, and $\phi(f,x) = |\phi(f,x)|\, \mathrm{e}^{\mathrm{i}\Theta(f,x)}$. A finite differential method can be used to estimate the spatially dependent variation of the spectrum:

$$\frac{\partial \phi(f,x)}{\partial x} = \lim_{\Delta x \to 0} \left(\frac{|\phi(f,x+\Delta x)| - |\phi(f,x)|}{\Delta x} \frac{1}{|\phi(f,x)|} + \mathrm{i} \frac{\Theta(f,x+\Delta x) - \Theta(f,x)}{\Delta x} \right) \phi(f,x). \tag{3}$$

Substituting Eq. (3) into Eq. (2), that is, solving $\phi(f,x+\Delta x)$ when Δx is very small, we obtain

$$\begin{aligned} \phi(f,x+\Delta x) = & \frac{\Lambda_f^L \cdot \Delta x + 1 - \mathrm{i}\left[\Theta(f,x+\Delta x) - \Theta(f,x)\right]}{\mathrm{e}^{-\mathrm{i}\left[\Theta(f,x+\Delta x) - \Theta(f,x)\right]}} \phi(f,x) \\ & + \frac{1}{2} \sum_{\substack{f_1,f_2 \\ f=f_1+f_2}} \frac{\Lambda_f^Q(f_1,f_2)\Delta x}{\mathrm{e}^{-\mathrm{i}\left[\Theta(f,x+\Delta x) - \Theta(f,x)\right]}} \phi(f_1,x)\phi(f_2,x), \end{aligned} \tag{4}$$

where $\Lambda_f^L = \gamma_f + \mathrm{i}\omega_f^-$.

Simplifying Eq. (4), we obtain

$$Y_f = L_f X_f + \sum_{\substack{f_1 \geq f_2 \\ f=f_1+f_2}} Q_f^{f_1,f_2} X_{f_1} X_{f_2}, \tag{1a}$$

where

$$\begin{aligned} & X_f = \phi(f,x) \quad Y_f = \phi(f,x+\Delta x), \\ & L_f = \frac{\Lambda_f^L \Delta x + 1 - \mathrm{i}\left[\Theta(f,x+\Delta x) - \Theta(f,x)\right]}{\mathrm{e}^{-\mathrm{i}\left[\Theta(f,x+\Delta x) - \Theta(f,x)\right]}}, \\ & Q_f^{f_1,f_2} = \frac{\Lambda_f^Q(f_1,f_2)\Delta x}{\mathrm{e}^{-\mathrm{i}\left[\Theta(f,x+\Delta x) - \Theta(f,x)\right]}}. \end{aligned}$$

Obviously, equation (1a) is essentially the same as Eq. (1), which is obtained by rewriting Eq. (2). Here, for convenience, the ε_f term is dropped for the time being and will be resumed bellow. Thus, the wave-coupling system is also described by input signal X_f and output signal Y_f. The input signal $x(t,x)$ and the output signal $y(t,x)$ are measured experimentally, and the input spectrum X_f and output spectrum Y_f can be obtained by Fourier transforming the input and output signals.

In the following algorithm, the digital bispectral analysis techniques will be employed to calculate the linear transfer function L_f and the quadratic transfer function $Q_f^{f_1,f_{21}}$ so that the corresponding output signal spectrum can be calculated from the new input signal spectrum, and thus the coupling coefficient and other derived physical quantities, such as the quadratic nonlinear energy transfer function, can be derived from these results.

2.2. Solution algorithm

To solve Eq. (1), the non-ideal effect needs to be corrected based on the "Kim *et al.*'s hypothesis" condition. The measured spectrum $\left(X_f, Y_f\right)$ is converted into the sum of ideal spectrum $\left(u_f, v_f\right)$ and a non-ideal spectrum $\left(X_f^{\mathrm{ni}}, Y_f^{\mathrm{ni}}\right)$ that does not participate in the wave coupling process:

$$X_f = u_f + X_f^{\mathrm{ni}} Y_f = v_f + Y_f^{\mathrm{ni}}. \tag{5}$$

The ideal spectrum here refers to the spectrum determined by the linear process and quadratic process described in Eq. (1). It can be assumed that the non-ideal spectrum $(X_f^{\mathrm{ni}}, Y_f^{\mathrm{ni}})$ is completely unrelated to the ideal wave spectrum $\left(u_f, v_f\right)$. It is worth noting that these two groups of spectra are independent of each other only if four-wave coupling and higher order process are much weaker than three-wave coupling. In this case, the third-order moment equations are obtained as follows:

$$\left\langle Y_f X_f^* \right\rangle = L_f \left\langle u_f u_f^* \right\rangle + \sum_{\substack{f_1 \geq f_2 \\ f=f_1+f_2}} Q_f^{f_1,f_2} \left\langle X_{f_1} X_{f_2} X_f^* \right\rangle, \tag{6}$$

$$\left\langle v_f v_f^* \right\rangle = L_f \left\langle X_f Y_f^* \right\rangle + \sum_{\substack{f_1 \geq f_2 \\ f=f_1+f_2}} Q_f^{f_1,f_2} \left\langle X_{f_1} X_{f_2} Y_f^* \right\rangle, \tag{7}$$

$$\begin{aligned} \left\langle Y_f X_{f_1}^* X_{f_2}^* \right\rangle = & L_f \left\langle X_f X_{f_1}^* X_{f_2}^* \right\rangle \\ & + \sum_{\substack{f_1 \geq f_2 \\ f=f_1'+f_2'=f_1+f_2}} Q_f^{f_1',f_2'} \left\langle X_{f_1'} X_{f_2'}^* X_{f_1}^* X_{f_2}^* \right\rangle. \end{aligned} \tag{8}$$

Here $\langle\cdot\rangle$ represents ensemble averaging, *i.e.*, statistical averaging on the parameters in brackets within the sample space. For the four variables L_f, $Q_f^{f_1,f_2}$, $\langle u_f u_f^* \rangle$, and $\langle v_f v_f^* \rangle$, another equation is needed to complete the equations system. For a fully developed turbulence, the time-static condition holds, namely, $\partial P_f / \partial x \approx (\langle v_f v_f^* \rangle - \langle u_f u_f^* \rangle)/\Delta x = 0$. Here, P_f is the power at frequency f. The fourth equation is thus obtained as follows:

$$\left\langle v_f v_f^* \right\rangle = \left\langle u_f u_f^* \right\rangle (= w_k), \tag{9}$$

where w_k refers to the frequency of the k-th sample, corresponding to frequency f, with $f = k\Delta f$. Equations (7)–(9) form a closed system, from which two expressions of linear transfer function L_k and a quadratic transfer function matrix $\boldsymbol{Q}(\equiv\{\boldsymbol{Q_k}\}, k = 1,2,\ldots,knum)$ can be obtained as follows:

$$L_k = \frac{\langle Y_f X_f^* \rangle - \left(\boldsymbol{B_k^*}\right)^{\mathrm{T}} \cdot \boldsymbol{F_k^{-1}} \cdot \boldsymbol{A_k}}{w_k - \left(\boldsymbol{A_k^*}\right)^{\mathrm{T}} \cdot \boldsymbol{F_k^{-1}} \cdot \boldsymbol{A_k}}, \tag{10a}$$

$$L_k = \frac{w_k - \left(\boldsymbol{B_k^*}\right)^{\mathrm{T}} \cdot \boldsymbol{F_k^{-1}} \cdot \boldsymbol{B_k}}{\langle X_f Y_f^* \rangle - \left(\boldsymbol{A_k^*}\right)^{\mathrm{T}} \cdot \boldsymbol{F_k^{-1}} \cdot \boldsymbol{B_k}}, \tag{10b}$$

$$\boldsymbol{Q_k} = \left(\boldsymbol{B_k^*}\right)^{\mathrm{T}} \cdot \boldsymbol{F_k^{-1}} - L_k \left(\boldsymbol{A_k^*}\right)^{\mathrm{T}} \cdot \boldsymbol{F_k^{-1}}. \tag{11}$$

Here, the vectors and matrices involved are defined by

$$\boldsymbol{Q_k} = \left(Q_k^{k/2,k/2}, Q_k^{(k+2)/2,(k-2)/2}, Q_k^{(k+4)/2,(k-4)/2}, \ldots, Q_k^{k_N,k-k_N}\right),$$
$$\boldsymbol{A_k} = (\langle X_{k/2}X_{k/2}X_k^*\rangle, \langle X_{(k+2)/2}X_{(k-2)/2}X_k^*\rangle, \langle X_{(k+4)/2}X_{(k-4)/2}X_k^*\rangle, \ldots, \langle X_kX_{k-k_N}X_k^*\rangle)^{\mathrm{T}},$$
$$\boldsymbol{B_k} = (\langle X_{k/2}X_{k/2}Y_k^*\rangle, \langle X_{(k+2)/2}X_{(k-2)/2}Y_k^*\rangle, \langle X_{(k+4)/2}X_{(k-4)/2}Y_k^*\rangle, \ldots, \langle X_kX_{k-k_N}Y_k^*\rangle)^{\mathrm{T}},$$
$$\boldsymbol{F}_k = \begin{bmatrix} \langle X_{k/2}X_{k/2}X_{k/2}^*X_{k/2}^*\rangle & \langle X_{k/2}X_{k/2}X_{(k+2)/2}^*X_{(k-2)/2}^*\rangle & \cdots & \cdots \\ \langle X_{(k+2)/2}X_{(k-2)/2}X_{k/2}^*X_{k/2}^*\rangle & \langle X_{(k+2)/2}X_{(k-2)/2}X_{(k+2)/2}^*X_{(k-2)/2}^*\rangle & \cdots & \cdots \\ \cdots & \cdots & \cdots & \cdots \\ \cdots & \cdots & \cdots & \langle X_{k_N}X_{k-k_N}X_{k_N}^*X_{k-k_N}^*\rangle \end{bmatrix}.$$

And here, we have defined $f = H(k)$, where H is a linear function and k is a constant number. That is, k is used as an index of frequency f, and is always an integer. In fully developed turbulence, it is approximately $f \approx k\Delta f$, and $\gamma_k \approx (|L_k|^2 - 1)/\Delta x$.

2.3. Programing

The programing flow of the specific algorithm is as follows.

Algorithm: Solver of wave coupling equations

Step 1 Original data: input signal $x(t,x), y(t,x)$;

Step 2 Pre-process:

Step 2.1 Defining and inputting assemble number (n), sample number (num),

Step 2.2 Performing Fourier transform on original data so as to get the source data set of input and output signal spectra X_i and $Y_i, i = 1,2,\ldots,N$;

Step 3 For $k = -num/2$ to $num/2-1$, the following steps are executed:

Step 3.1 Calculating all groups (k_1,k_2) that satisfy the condition '$k_1+k_2=k$', and saving the group number as $knum$,

Step 3.2 computing array $\boldsymbol{A_k}$, $\boldsymbol{B_k}$, and the matrix $\boldsymbol{F}_k$,

Step 3.3 Computing $L_k, \boldsymbol{Q_k}$,

Step 3.4 Computing the linear coupling coefficient and assigning it to the array $\Lambda_f^L(k)$,

Step 3.5 Calculating the quadratic coupling coefficient $z(1\ldots knum)$ and assigning it to the array $\Lambda_f^Q\ (k, 1\ldots knum)$,

Step 3.6 Calculating the power transfer function $T_f\,(f_1,f_2)$;

Step 4 Calculating the nonlinear energy transfer function W_{NL}^f;

Step 5 Outputting L_f and $Q_f^{f_1,f_2}$, Λ_f^L and Λ_f^Q, T_f and W_{NL}^f.

Here two issues need to be addressed. First, the parameters k, k_1 and k_2 should meet the three-wave coupling condition $k = k_1 + k_2$, and the determination of these indicators is one of the basic points for this program.[14] Secondly, the ensemble number (n) and sample number (num) should be big enough to ensure the accuracy of spectrum estimation. In a fully developed turbulence system, $n \geq 1000$ and $num \geq 64$ are generally taken, and the number of samples overlapped for each realization segment takes $np \sim num/2$, or the total number of sampled data meets the condition $n \times (num - np) + np > 3 \times 10^4$. Also, num must be an exponential multiple of 2; or, in the Fourier transform, fill some numbers '0' in sample data set to meet this requirement.

The pre-processing of input and output data is described below. Taking the study of edge plasma turbulence in tokamak for example,[13] we take the float potentials as the original signals, obtaining at two adjacent spatial points in poloidal direction during the period of [600, 700] ms in an experimental discharge, with a sampling frequency of 1 MHz and thus the Nyquist frequency of 500 kHz. There are two groups of sample data. The first set of data (corresponding to the first spatial point) serves as the input signal and the second set (corresponding to the second point) as the output signal. We can take 780 realizations ($n = 780$) and 256 samples ($num = 256$) for each realization. It is worth noting that the sampled data need to be partially overlapped. The number of overlapping samples for each realization can be $np = 128$, thus the total number of source data required for each channel is $(num - np) + np = 99968 < 10^5$; and it is obvious that the practically total number of sample data can meet this requirement. Subsequently, the Fourier transform can be performed on the data for each realization to obtain the input and output signal spectra, which will be used as the input and output data in the program.

The third step is the core of the program, which is actually the solver for Eq. (1) or Eq. (1a). In addition, if the program is used for energy transfer analysis of turbulence, it is necessary to calculate nonlinear energy transfer function, that is,

$$W_{\mathrm{NL}}^f = (1+(f/\Delta f)^2) \sum_{\substack{f_1,f_2 \\ f=f_1+f_2}} T_f(f_1,f_2), \tag{12}$$

where $T_f(f_1,f_2)$ is the power transfer function calculated in the program, defined as follows:

$$T_f\,(f_1,f_2) = \mathrm{Re}\left[\Lambda_f^Q\,(f_1,f_2)\left\langle \phi_f^*\phi_{f_1}\phi_{f_2}\right\rangle\right]. \tag{13}$$

The power transfer function represents the power change in the wave with the frequency f in the wave coupling process ($f = f_1 + f_2$). The nonlinear energy transfer function W_{NL}^f represents the variation of the nonlinear energy of wave with frequency f.

3. Simulation

3.1. Simulation data generation

To simulate the fully developed turbulence and testify the program, the simulation data are generated in the following. Firstly, a nonlinear system model needs to be created, namely, the linear coupling coefficients Λ_f^L and the quadratic coupling coefficients $\Lambda_f^Q(f_1,f_2)$ should be pre-defined. And then, the spectra of white Gaussian noise are used as the input signal spectra, and the output spectra are then obtained through the pre-defined turbulence model. In the simulation analysis, the condition "Kim *et al.*'s hypothesis" can be so simplified that for a nonlinear system with input spectrum generated by colored noise spectrum, its output spectrum is equal to its input spectrum.[8,11] In order to make the simulation analysis representative, we generate the fully developed turbulence model based on Hasegawa model.[22,23] The values of average dispersion relation $\omega_k(\equiv \mathrm{Im}\left(\Lambda_k^L\right))$ and quadratic nonlinear coupling coefficient $\Lambda_k^Q(k_1,k_2)$ are thus defined as follows:

$$\omega_k = 0.5k/\hat{k}, \tag{14a}$$

$$\Lambda_k^Q(k_1,k_2) = \frac{20}{\hat{k}^4}k_1k_2\left(k_2^2-k_1^2\right)/\left(1+k^2/\hat{k}^2\right), \tag{14b}$$

where k is defined as the index of frequency f as mentioned above, which approximately satisfies the relation $f = k\Delta f$ and three-wave coupling condition, namely $f = f_1+f_2$, or say, $k = k_1+k_2$. And for simplicity, we take $\hat{k} = 32$, and $\Delta f = 1$ kHz.

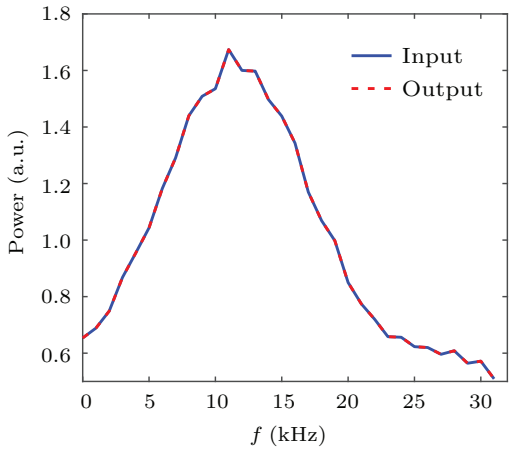


Fig. 2. Auto-power spectrum of input signal and output signal.

In the simulation, the original input data are white Gaussian noise signals, which pass through the "black box" 12 times, and the output signal of the last black box serves as the final input signal to simulate a fully developed turbulence. Its power spectrum is shown in solid blue lines in Fig. 2. And then, according to the given mean dispersion relation (Eq. (14a)), the quadratic nonlinear coupling coefficient (Eq. (14b)), and the constraint conditions $\langle Y_kY_k^*\rangle = \langle X_kX_k^*\rangle$, the output signals are simultaneously obtained, and their power spectrum is plotted by the red dot line in Fig. 2. Thirdly, under the constraint of $\langle Y_kY_k^*\rangle = \langle X_kX_k^*\rangle$, the corresponding (also seen as "pre-setting" values) linear growth rate $\gamma\ (\equiv \mathrm{Re}(\Lambda_k^L))$ of the turbulence model can be obtained as shown in Fig. 3(a). Figure 3(b) shows the average dispersion relation pre-setting values in Eq. (14a). Plotted in Fig. 3(c) is the mode of the quadratic nonlinear transfer function, $\left|Q_f(f_1,f_2)\right|$, which is converted from the quadratic nonlinear coupling coefficient Λ_k^Q.

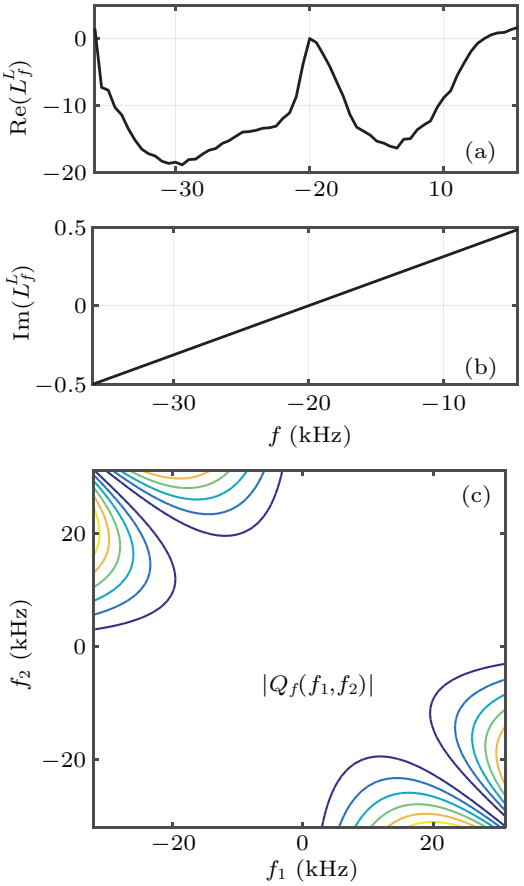


Fig. 3. Pre-setting values of nonlinear system model: (a) real part of Λ_f^L, (b) imaginary part of Λ_f^L, and (c) the mode of quadratic nonlinear transfer function.

As seen from Figs. 3(a) and 3(b), the real part of the linear coupling coefficient (corresponding to the growth rate γ) is basically symmetric about the axis $x = 0$, while its imaginary part (corresponding to the mean dispersion function) is symmetric about the origin point.

3.2. Comparison and analysis of simulation results

The ideal turbulence model that satisfies Kim *et al.*'s hypothesis has been defined above. The input and output spectrum signals generated are input in the present program for computations, and then the calculated phase spectrum, linear and quadratic coupling coefficients, and the estimated

quadratic transfer function, are obtained and illustrated in Fig. 4. Note that the real part of the linear coupling coefficient Λ_f^L is also the linear growth rate γ, and its imaginary part is the average dispersion relation ω_r^-.

As seen from Fig. 4(a), since the ideal output spectrum Y_k is calculated from the input signal spectrum X_k according to the constraint condition $\langle Y_k Y_k^* \rangle = \langle X_k X_k^* \rangle$, the phase difference between the output signal spectrum Y_k and the input signal spectrum X_k is not smooth, while this does not weaken the correctness of the simulation results. Comparing Fig. 4(c) with Fig. 3(a), as well as comparing Fig. 4(b) with Fig. 3(b), it is demonstrated that the real part and the imaginary part of Λ_f^L calculated are basically equal to the pre-setting values within a certain error range. And the mode of the nonlinear transfer function, $\left|Q_f(f_1, f_2)\right|$, as shown in Fig. 4(d), is approximately identical with that in Fig. 3(c). All these results confirm that the program runs well.

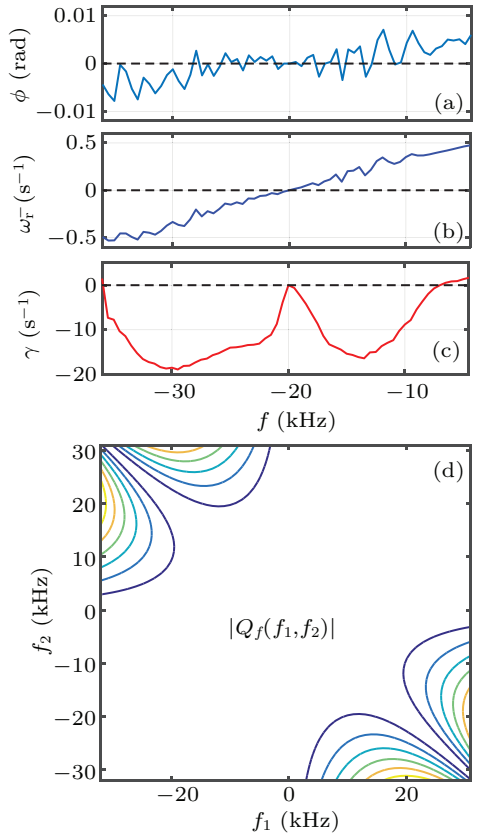


Fig. 4. Results of calculations from program: (a) phase ϕ, (b) average dispersion ω_r^-, (c) linear growth rate γ, and (d) mode of quadratic nonlinear transfer function.

Plotted in Fig. 5 is the comparison between the linear growth rate γ_f calculated and $T_f/2P_f$. Obviously, it indicates the relationship $\gamma_f - T_f/2P_f \approx 0$, suggesting that

$$\frac{\partial P_f}{\partial t} \equiv 2\gamma_f P_f - T_f \approx 0,$$

namely, as the difference between the input power and the output power satisfies $\Delta P_f \equiv P_f(x+\Delta x) - P_f(x) \approx 0$, indicating an approximately constant power. It can be shown that the output spectrum here belongs to the ideal output spectrum, the model meets Kim *et al.*'s hypothesis, so it is suitable for the algorithm in this paper, and the program running results are physically accurate.

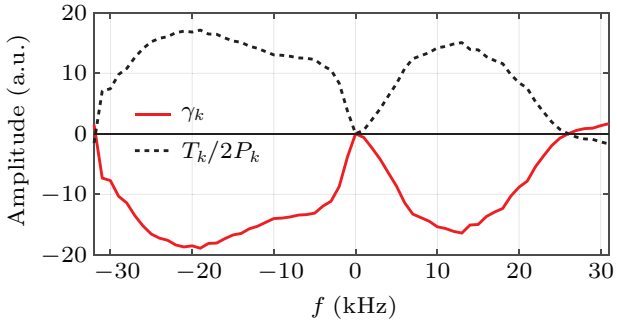


Fig. 5. Comparison between linear growth rate γ_f and $T_f/2P_f$.

4. Application: Case calculation

The study of plasma in a toroidal device involves with many aspects.[25–28] Here we choose the edge plasma turbulence data measured in an experiment on the toroidal device, and employ the present program to calculate and analyze the energy transfer in the turbulent system, so as to test the efficiency of the algorithm and program in practical application. Shown in Fig. 6 is the signals evolve with time in the input channel and the output channel in Discharge 53441 on TPE-RX RFP device. The sampling frequency is 1 MHz. The measured 3.1×10^4 data in total in a range from $t = 18.5$ ms to 49.5 ms are taken as the original signals. The number of realizations is taken to be $n = 480$, and the number of samples at a time is $num = 128$, and the number of overlapped samples in each segment is taken $np = 64$. Hence, the total number of sample data required for each channel is 30784 (< 31000).

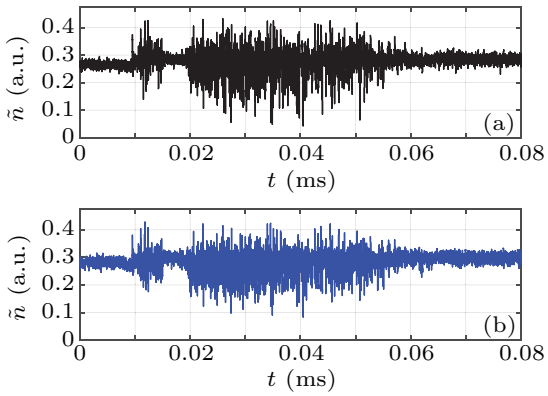


Fig. 6. Signal amplitude diagram of (a) input channel and (b) output channel in turbulence experiment.

The input and the output power spectra are shown in Fig. 7. For this experimental edge plasma turbulence, clearly most of the energy is concentrated in the lower frequency region. In this system, the auto-power spectrum reaches its max-

imum value at $f = 0$ kHz, about 3 a.u., and most of the energy is concentrated within the range of $f < 100$ kHz.

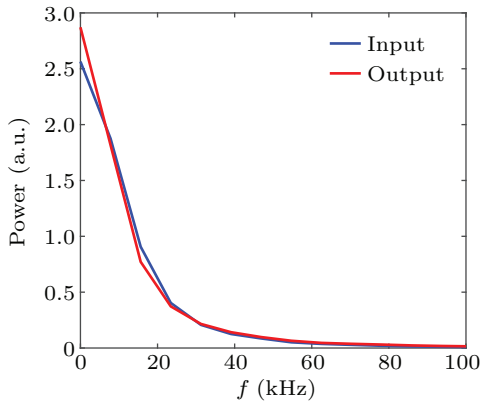


Fig. 7. Auto-power of input signal spectrum and output signal spectrum in turbulence experiment.

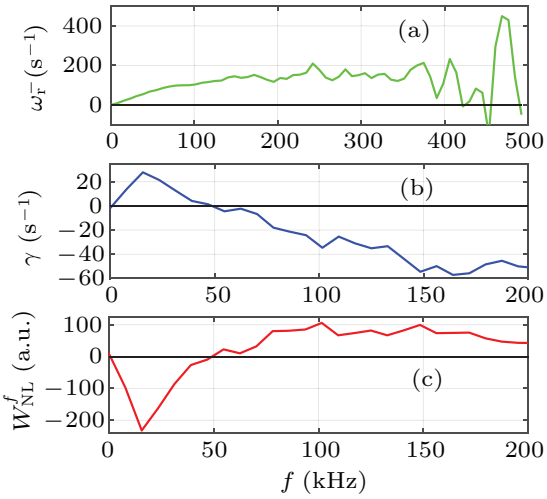


Fig. 8. Calculated results of (a) average dispersion ω_r^-, (b) linear growth rate γ, (c) quadratic nonlinear energy transfer function (W_{NL}^f).

The above data are pre-processed, the input signal spectrum and the output signal spectra are input in the system, and the present program was run. As a result, the estimated results of linear and quadratic nonlinear coupling coefficient are obtained as shown in Fig. 8. It should be noted that in this algorithm, the positive frequency represents the wave propagating along the forward direction, and the negative frequency indicates the wave propagating along the opposite direction. The values of the growth rate γ and the nonlinear energy transfer function W_{NL}^f in the region of $[-200, 0]$ kHz are not plotted, and in fact, their values are even symmetric with respect to the corresponding values of [0, 200] kHz. This can be clearly seen in Fig. 9 below. By analyzing the results, we see that the average dispersion relation ω_r^- changes continuously, and the output signals are obviously generated from the input signals through the nonlinear system. Figure 8(b) shows the distribution of linear growth rate γ in the spectrum space. In the frequency range of $f > 50$ kHz, there is $\gamma < 0$, indicating that the turbulence wave in this frequency band damps. While $\gamma > 0$ holds for $0 < f < 50$ kHz, the turbulent wave grows linearly in this region. Figure 8(c) shows that for $f > 50$ kHz, there is $W_{NL}^f > 0$, indicating that the turbulent wave in this frequency range can receive energy. However, in the region of $[0,\ 50]$ kHz, $W_{NL}^f < 0$ holds, meaning that the turbulence loses energy. Hence, this creates a physical picture of energy transfer in this fully developed turbulence. Figures 8(a)–8(c) show that the energy in this turbulence is transferred from lower frequency region to higher frequency region and the corresponding wave turns from a linear growing wave to a damping wave.

Figure 9 shows the variation of growth rate and the power change with frequency. It is demonstrated that in the frequency interval $f \in [0, 200]$ kHz, γ_f and $T_f/2P_f$ are symmetric about the real axis, *i.e.* $\partial P_f/\partial t \equiv 2\gamma_f P_f - T_f \approx 0$, indicating that the output signal is an ideal output spectrum signal obtained by the input signal spectrum through a quadratic nonlinear system, meaning that it is appropriate to apply this algorithm to it. Reviewing Fig. 7, since the spectrum power of the system concentrates mainly in lower frequency region and the power difference in higher frequency region can be ignored, the whole system meets the ideal output spectrum condition. Furthermore, by reexamining Fig. 8, it is seen that the linear growth rate γ exactly matches the change of the quadratic nonlinear energy transfer function W_{NL}^f, indicating that the calculated linear growth rate and quadratic nonlinear coupling coefficient are reasonable.

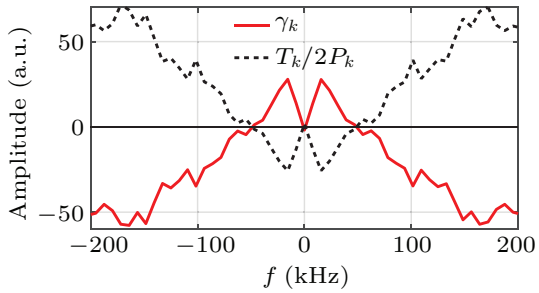


Fig. 9. Variation of growth rate and power change with frequency.

The auto-power spectra of the input signal and output signal shown in Fig. 7 are very similar, but there are still differences, which are the basic characteristics of the wave when the three-wave coupling predominates in the edge plasma turbulence. If such differences are small enough, the computational results are reliable; however, if the difference is too large, or say, the two auto-power spectra are not very similar, indicating that much useful information about spectrum would be lost when separating the non-ideal spectrum from ideal one, the computational results seem not precise as discussed in detail in Ref. [11].

In addition, the coherence of turbulence at two spatial points can affect the calculation results. In order to avoid such adverse effects, it is required to make the two spatial points where the input and output signals are measured close enough, that is, the value of Δx should be small enough. Generally, in a medium-sized toroidal device, the accuracy can be guaranteed by selecting $\Delta x \sim 0.1$ cm–0.5 cm.

5. Summary

In this paper, a nonlinear wave coupling algorithm is proposed and implemented by a program. The algorithm is based on digital bis-spectrum estimation analysis and Kim *et al*.'s hypothesis,[9] that is, it is assumed that the input signal spectral power is equal to the output spectral power. Shen *et al*. have compared Kim *et al*.'s method with the complete iterative method[12] and proposed that Kim *et al*.'s method is more suitable for the analysis of energy transfer in edge plasma turbulence. The algorithm in this work belongs to Kim *et al*.'s method in essence.

In this algorithm, the nonlinear energy transfer function is calculated directly from the wave coupling coefficients, thereby improving the computation accuracy. When we apply the algorithm to the identification of turbulent energy transfer process, the original algorithm is transformed from wave-number space into frequency space, which is appropriate to the physical characteristics of edge plasma turbulence.[29] The programing flow is given, and the simulation analysis is carried out, showing that the calculation results are reliable. As an application, the energy cascade analysis of typical edge plasma turbulence is performed. As a result, a physical picture of the energy transfer in the turbulent system is constructed, confirming that the energy transfer in this turbulent system spreads from lower- to higher-frequency region and its corresponding wave turns from a linear growing wave into a damping wave. The case analysis also demonstrates that the algorithm and program are both suitable to the study of the fully developed turbulence or saturated turbulence, such as edge plasma turbulence.[18,19]

Acknowledgements

Project supported by the National Key Research and Development Program of China (Grant No. 2017YFE0301200), the National Natural Science Foundation of China (Grant Nos. 12075077 and 12175055), and the Science and Technology Project of Sichuan Pprovince, China (Grant No. 2020YJ0464).

References

[1] Buzzicotti M, Aluie H, Biferale L, *et al*. 2018 *Phys. Rev. Fluids* **3** 034802
[2] Harper K L and Nazarenko S V 2016 *New J. Phys.* **18** 085008
[3] Shi Z B, Nagayama Y, Yamaguchi, *et al*. 2011 *Phys. Plasmas* **18** 102315
[4] Shen Y, Dong J Q and Xu H B 2018 *Acta Phys. Sin.* **67** 195203 (in Chinese)
[5] Xia H and Shats M G 2003 *Phys. Rev. Lett.* **91** 155001
[6] Ritz C P and Powers E J 1986 *Physica D* **20** 320
[7] Ritz C P, Powers E J, Miksad R W, *et al*. 1988 *Phys. Fluids* **31** 3577
[8] Ritz C P, Powers E J and Bengsten R D 1989 *Phys. Fluids B* **1** 153
[9] Kim J S, Durst R D, Fonck R J, *et al*. 1996 *Phys. Plasmas* **3** 3998
[10] Kim K I, Powers E J, Ritz C P, *et al*. 1987 *IEEE J. Ocean Eng.* **OE-12** 568
[11] Shen Y H, Li J Y, Li T, *et al*. 2020 *Phys. Scr.* **95** 055202
[12] Shen Y H, Li J and Li T 2020 *J. Phys. Soc. Jpn.* **89** 044501
[13] Shen Y, Dong J Q, Shi Z B, *et al*. 2015 *Nucl. Fusion Plasma Phys.* **35** 193 (in Chinese)
[14] Shen Y, Dong J Q, Shi Z B, *et al*. 2017 *Nucl. Fusion Plasma Phys.* **37** 1 (in Chinese)
[15] Schmid B, Manz P, Ramisch M, *et al*. 2017 *Phys. Rev. Lett.* **118** 055001
[16] Cziegler I, Hubbard A E, Hughes J W, *et al*. 2017 *Phys. Rev. Lett.* **118** 105003
[17] Manz P, Ramisch M, Stroth U, *et al*. 2008 *Plasma Phys. Control. Fusion* **50** 035008
[18] Manz P, Ramisch M and Stroth U 2009 *Phys. Rev. Lett.* **103** 165004
[19] Shen Y, Dong J Q, Shi Z B, *et al*. 2019 *Nucl. Fusion* **59** 044001
[20] Xu M, Tynan G R, Diamond P H, *et al*. 2012 *Phys. Rev. Lett.* **108** 245001
[21] Zhao K J, Lan T, Dong J Q, *et al*. 2006 *Phys. Rev. Lett.* **96** 255004
[22] Hasegawa A and Wakatani M 1987 *Phys. Rev. Lett.* **59** 1581
[23] Hasegawa A and Mimma K 1978 *Phys. Fluids* **21** 87
[24] Jones F L, Ritz C P, Miksad R W, *et al*. 1988 *Exp. Fluids* **6** 365
[25] Chen W, Cui Z Y, Sun P, *et al*. 2007 *Chin. Phys.* **16** 3451
[26] Shen Y, Dong J Q, He H D, *et al*. 2021 *Acta Phys. Sin.* **70** 185201 (in Chinese)
[27] Zhou Y L, Wang Z H, Xu M, *et al*. 2016 *Chin. Phys. B* **25** 095201
[28] Wu X K, Wang Z H, Li H D, *et al*. 2020 *Chin. Phys. B* **29** 065201
[29] Zhao K J, Dong J Q, Yan L W, *et al*. 2007 *Phys. Plasmas* **14** 122301